

Aerodynamic optimization of a large PrandtlPlane configuration *

L. Cappelli, G. Costa, V. Cipolla, ^a A. Frediani, ^a, F. Oliviero, ^a, E. Rizzo

^aUniversity of Pisa, Department of Civil and Industrial Engineering

Abstract

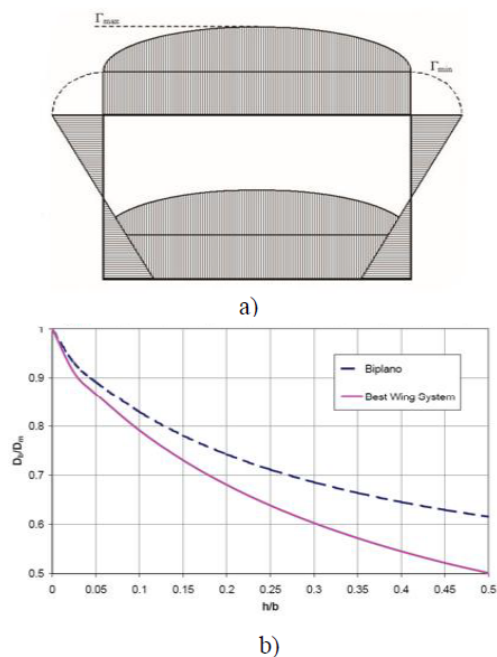
The purpose of this paper is to present design procedures and tools for the aerodynamic optimization of a large freighter aircraft with a PrandtlPlane configuration. Suitable optimization tools have been developed and are shortly described in the paper; sensitivity analyses for high speed flight conditions have been performed, and, also, low speed performances are evaluated to provide a complete preliminary design of the PrandtlPlane freighter.

1. Nomenclature

α	=	Angle of attack
δ_e	=	Elevator deflection angle
δ_f	=	Flap deflection angle
ω_{sp}	=	Short-period mode frequency
b	=	Wingspan of the box-wing system
C_D	=	Drag coefficient
C_L	=	Lift coefficient
C_m	=	Pitch moment coefficient
CG	=	Center of Gravity
D	=	Drag force
E	=	Aerodynamic efficiency (L/D)
h	=	Height of the box-wing system
k_{bulk}	=	bulk parameter
l_{bulk}	=	tip-wing (“bulk”) length
L	=	Lift force
mac	=	Mean aerodynamic chord
m_q	=	Pitch moment vs pitch angular rate derivative
m_α	=	Pitch moment vs α derivative
M	=	Mach number
$MTOW$	=	Maximum Take-Off Weight
Re	=	Reynolds number
S	=	Wing area
SM	=	Longitudinal Stability Margin
V	=	Flight speed
\vec{x}	=	Optimization variables vector
W	=	Weight
OEW	=	Operating empty weight
Z_w	=	Vertical force vs vertical speed derivative

2. Introduction

The PrandtlPlane configuration originates from L. Prandtl’s studies on the “best wing system” (BWS) concept ([1]), which consists in a box-wing in the front view, designed in such a way that the total lift is the superposition of a constant and an elliptic distribution in the horizontal wings and a butterfly-shaped distribution on the vertical tip-wings, called hereafter “bulks” (Figure 1-a).



*The present paper has been presented at the 23rd Conference of AIDAA, the Italian Association of Aeronautics and Astronautics, held in Turin (Italy) on 17-19 November 2015

¹©AIDAA, Associazione Italiana di Aeronautica e Astronautica

Figure 1. The Best Wing System

(Figure 1-b), from [2], shows the induced drag of the BWS and the optimum biplane, as percentage of the induced drag of the optimum monoplane vs the nondimensional gap (vertical gap/wing span). It is remarkable that the best wing system is more efficient than the optimum biplane in terms of induced drag and, also, is 20-30% more efficient than the optimum monoplane. The PrandtlPlane configuration can be adopted to design any dimension aircraft, from very small to extra large, much bigger than the conventional monoplanes. In recent times, an increasing interest is devoted to the improvement of air transport and the PrandtlPlane configuration could be a solution also for very large aircraft, as shown in this paper.

This work deals with the optimization of a PrandtlPlane freighter, starting from a configuration similar to the one represented in Figure 2.

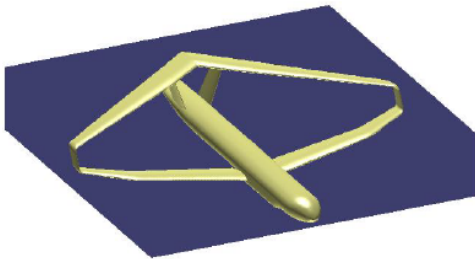


Figure 2. Example of PrandtlPlane freighter

The main characteristics and the advantages of the PrandtlPlane configuration have been discussed in previous works ([2], [3], [4], [5], [6], [7]) showing also the possible disadvantages and, in particular, flutter characteristics. The particular aspects to be faced in the case of a very large freighter regard the interaction between structures and Flight Mechanics and Controls.

The bending and torsional stiffness of the wing structures, contrary to cantilever wings, are strongly influenced by the overconstrained connections to the fuselage. Also the structural solutions of the lifting system are totally innovative because, in principle, it is possible to obtain distributions of bending and torsional moments not correlated with the lifting forces. The structural design of the fuselage can be innovative as well, as shown later on. Flight Mechanics and Controls are different from those of cantilever wings. In the present proposal, all the wings undergo positive lifts. Longitudinal Stability with a given margin is a constraint of the optimization and the influence of this constraint will be underlined in this paper. The design of the aerodynamic controls of a PrandtlPlane is totally different from conventional aircraft and, taking

the large inertia along the pitch axis into account, the pitch control needs to be very powerful; the requirements of Flight Dynamics in a very large PrandtlPlane freighter are a real challenge.

The PrandtlPlane configuration can overcome these difficulties; in particular, the requirements on the longitudinal stability and dynamics are satisfied with a reduced longitudinal Stability Margin ($SM = 0-3\%$), lower than conventional (10-15%): in fact, the m_q derivative is higher in PrandtlPlane aircraft and it affects the short period frequency ($\omega_{sp} = \sqrt{-m_\alpha + Z_w + m_q}$). Good flight qualities need a proper range of ω_{sp} and hence, being m_q high and negative, the only way to reduce the value of ω_{sp} is to reduce m_α , that is to reduce the Stability Margin. The architecture of the longitudinal control system is based on the presence of elevators positioned as far as possible each other in the aircraft and moved in phase opposition.

Lateral control is obtained by ailerons positioned at all the wing tips and, thus, is very efficient; lateral stability is a critical item due to the rearward shift of the centre of gravity; twin fins are mandatory to face the problems of dynamics of structures and flutter.

The aim of this paper is limited to present only the methodologies adopted to design a PrandtlPlane in the particular case of a very large freighter. The freighter is properly designed in order to transport intermodal containers; the aircraft is much bigger than any existing one but, at the same time, the overall dimensions are included in a square of 80 x 80 m plane, to be compatible with the present airport areas.

According to [8], the relevant features of the proposed PrandtlPlane freighter are presented in Table 1.

Some of the main characteristics of the fuselage can be found in the sketch in Figure 3 the fuselage is enlarged horizontally in order to host a 20ft container. The containers are loaded and unloaded through two doors, in the front and rear fuselage, and are moved longitudinally inside. No pressurization neither windows are needed.

In this work, a third lifting surface has been introduced in order to enlarge the set of the feasible solutions with the aim of improving maneuverability and reducing the fuselage stress; a preliminary sketch of the configuration is shown in Figure 4. A third lifting surface (called "auxiliary wing" in this paper) implies advantages and drawbacks. On one hand, there is a weight increase due to the presence of the third wing but, on the other hand, there is a weight saving on the fuselage and an easier maneuverability at low speed.

The empty weight saving of the fuselage is a great potential advantage of this solution; in fact the fuselage is now equivalent to a three-supported beam instead of a cantilever one. The auxiliary wing is positioned far from the aircraft center of gravity in order

Table 1
PrandtlPlane freighter features

DESIGN PARAMETERS	
Fuselage Length	80 m
Cruise Mach	0.65
Wingspan	80 m
Cruise Altitude	6000 m
Range	3000 nm
Max Runway Length	4000 m
Engines	Open Rotors
Number of containers	25
WEIGHT ESTIMATE	
$MTOW$	624883 kg
OEW	250420 kg (40.1%)
W_{fuel}	124460 kg (19.4%)
$W_{payload}$	250000 kg (40.5%)

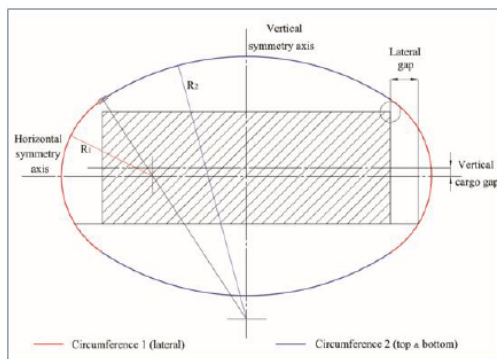


Figure 3. Typical PrandtlPlane freighter fuselage cross section

to maximize the stability and controllability effects.

The structural solution of the fuselage is based on the favourable positions of the aerodynamic supports in Figure 4. As an example, we assume the material properties, section properties, and loads from [8], summarized in Table 2 and Figure 4 is taken as an initial configuration.

In the case of an auxiliary lifting wing positioned in the nose of the aircraft, a possible reduction of bending moments can be trivially deduced from Figure 5; this example is only qualitative because the trim conditions are unknown. In the following of the paper, we analyze the optimization process of the aircraft configuration; this process is the result of a long research activity in which the optimization tools were set up and verified with very positive results. The

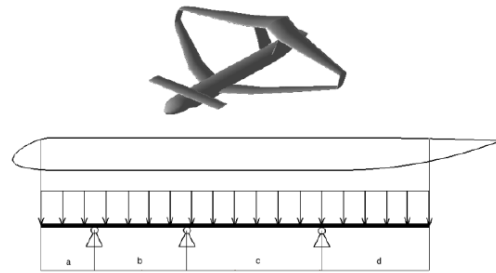


Figure 4. The auxiliary wing on the PrandtlPlane freighter

Table 2
Main quantities

Young Modulus [MPa]	73000
Total Length [mm]	64000
Section Moment of Inertia [mm ⁴]	$4.69 \cdot 10^{11}$
Distributed Load [N/mm]	102.5

design process includes the use of a surface generator *ASD* (Aerodynamic Shape Designer, [9] [10]) and the aerodynamic optimizer *AEROSTATE* (AERodynamic Optimization with STatic stability and Trim Evaluator, [11] [12]), both developed with Matlab at the Aerospace Engineering Department of the Pisa University. The optimization tools were modified and extended, in order to optimize the aircraft with the auxiliary wing.

3. Shape design of freighter aircraft

ASD allows us to shape a complex surface in a parametric, quick and modular way. The generation of aerodynamic surfaces is carried out by the interpolation of N.U.R.B.S. curves. Conventional and non conventional configurations can be represented and quickly changed during an optimization process. *ASD* allows to edit external and internal aerodynamic shapes, axis-symmetric bodies, bulks and fillet surfaces, etc.

4. The optimization tool *AEROSTATE*

AEROSTATE is another in-house software and its theoretical basis are described in [11] and [12]. It allows us to find the optimum wing planforms of any configuration under geometrical and aerodynamic constraints in cruise condition. The research of the optimum configuration in *AEROSTATE* is obtained by the implementation of a local and a global algorithm.

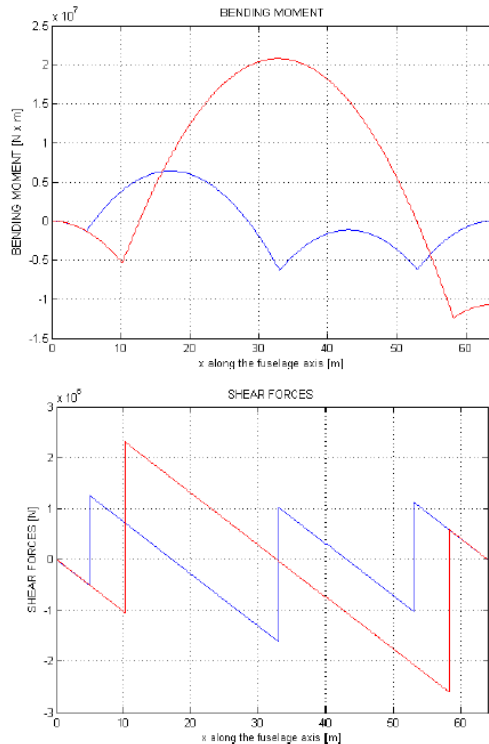


Figure 5. Qualitative comparison between bending moments and shear forces

There are two basic strategies to determine the optimum of a constrained or an unconstrained function: the first one is an analytic exact method, which computes the Hessian matrix to evaluate the gradient of the function; the second strategy uses algorithms which contain a random component (e.g. genetic), and it is based on the so-called “heuristic methods”. Analytic methods can find out the local minimum, while heuristic methods determine the global minimum, sacrificing the solution speed. The present problem has many variables, many constraints and the objective function cannot be evaluated in the analytic way: if a gradient method is used, probably the solution tends to a local minimum and not to the global one. Genetic algorithms are not efficient from a computational point of view, thus, the present algorithm is composed of a local algorithm to find out local minima and of a procedure to build an approximation of the objective function.

The local algorithm implemented in *AEROSTATE* is the SQP (Sequential Quadratic Programming) Method. The global algorithm in this software is called *LOCSMOOTH* (Local Optima Smoothing for Global Optimization).

4.1. Optimization methods and software structure

Given a set of parameters \vec{x} and defined the objective function $f(\vec{x})$, inequality and equality constraints, respectively $g(\vec{x})$ and $h(\vec{x})$, such as:

$$\begin{aligned} \mathbf{f} : \mathbb{R}^n &\rightarrow \mathbb{R}, & \mathbf{f} &\in \mathbf{C}^1 \\ \mathbf{g} : \mathbb{R}^n &\rightarrow \mathbb{R}^p, & \mathbf{g} &\in \mathbf{C}^1 \\ \mathbf{h} : \mathbb{R}^n &\rightarrow \mathbb{R}^m, & \mathbf{h} &\in \mathbf{C}^1 \end{aligned} \quad (1)$$

the optimization problem has the following mathematical formulation:

$$\begin{cases} \min f(\vec{x}) \\ \vec{x} \in \Omega \subset \mathbb{R}^n \end{cases} \quad (2)$$

where the set Ω is defined as follows:

$$\Omega = \{ \vec{x} \in \mathbb{R}^n : g(\vec{x}) \leq 0, h(\vec{x}) = 0 \} \quad (3)$$

The SQP algorithm can be considered an extension of the Newton’s method to the constrained optimum problem. The basic idea is to move away from the current point by minimizing a quadratic model of the problem. The SQP method has been implemented in the optimizer (*AEROSTATE*) by means a dedicated Matlab function and its aim is to find out local minima ([11]). The *LOCSMOOTH* algorithm is used to determine the global minimum of the objective function (e.g. the curve represented in continuous line in Figure 6).

This algorithm works properly when the starting function has a funnel structure, i.e. a superposition of an underlying structure (the dashed curve represented in Figure 6) and some perturbation around it.

The local optimum, said \vec{x}_1^* , depends on the starting point \vec{x}^* ; thus, the local optimum function $L(\vec{x}^*)$ can be defined and reported in Figure 6 with the tick line: this is a step function and rapid convergence algorithms cannot be applied. For this reason, a Gaussian filtering smooths the thickest curve and the minimum point of the smoothed function is found. From this point, the local minimum of the objective function is searched with SQP algorithm.

The Matlab functions which compose *AEROSTATE* are described in [11] and in [12]. In this section, it is explained how the aerodynamic problem is set in *AEROSTATE*. All the variable of the optimization problem are collected in the array x and they are indicated in Figure 7. The front and the rear wings are divided in two bays by three control sections, while the auxiliary wing is constituted by one bay, limited by two control sections. The pitch angle can be a variable or a constant. The bulk is automatically generated by means the geometric parameters on the tip of both the two wings. The lower and the upper boundaries of the variables are collected respectively in the arrays $\vec{l}\vec{b}$ and $\vec{u}\vec{b}$, and they define the set Ω of definition of the problem ($\vec{l}\vec{b} < \vec{x} < \vec{u}\vec{b}$).

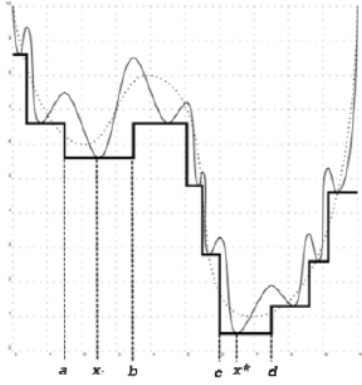


Figure 6. Objective function - LOCSMOOTH algorithm

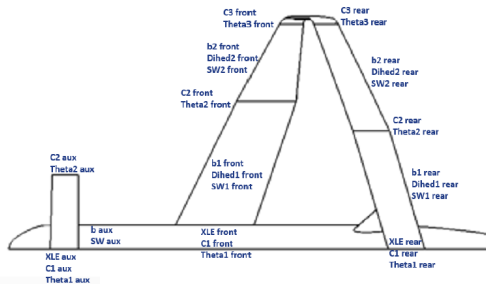


Figure 7. Optimization variables

The objective function takes the aerodynamic efficiency and the bulks length (l_{bulk}) into account. This latter, which has to be low because of structural buckling, is multiplied to the empirical coefficient k_{bulk} , called “bulk parameter”. Therefore, the optimization problem is specified for the PrandtlPlane as follows:

$$\begin{cases} \min f(\vec{x}) = \min(-E + k_{\text{bulk}}l_{\text{bulk}}) \\ g(\vec{x}) \leq 0 \\ \vec{x} \in \Omega \subset \mathbb{R}^n \end{cases} \quad (4)$$

$$\begin{cases} |L_{\text{tot}} - W_{\text{desing}}| \leq \epsilon W \\ m_{CG} \leq \epsilon_m \\ SM_{\min} \leq SM \leq SM_{\max} \\ W/S_{\min} \leq W/S \leq W/S_{\max}, \text{ for each wing} \\ C_L \leq C_{L_{\max}}, \text{ for each wing} \\ |geom(\vec{x}) - constr(\vec{x})| \leq \epsilon_g \end{cases} \quad (5)$$

The first two relationships are the equilibrium to the pitch moment and to the vertical translation, whereas the third one represents the limitations applied for the Stability Margin (SM). The following two expressions

are constrains in terms of wing loading (W/S) and maximum lift coefficient (C_L) of each wing, and, finally, the last expression introduces some geometric constraints to the aircraft shape.

4.1.1. The software AVL

Athena Vortex Lattice (AVL, [13]) is a program for the aerodynamic and flight-dynamic analysis of rigid aircraft of arbitrary configuration. It employs an extended vortex lattice model for the lifting surfaces, together with a slender-body model for fuselages and nacelles.

AVL is the aerodynamic software used by *AEROSTATE* because it is fast and simple to manage; it is reliable in subsonic linear field, induced drag is well evaluated and stability and trim results are provided. The only drawback is that non-lifting bodies (i.e. the fuselage) are difficult to be included in the computation. As done in previous works, such as [14] and [15], this problem can be faced by modeling the fuselage as a lifting surface, continuously connected to the front wing, whose planform is the top view of the fuselage.

The lateral stability and maneuverability are not considered and two vertical fins are assumed to meet all constraints. The symmetry conditions allow to model only half configuration: thus, aerodynamic lifting coefficients need to be scaled during the analysis of results.

The friction drag coefficient (C_{D0}) is evaluated: the friction drag contribution of the fuselage is computed with the flat sheet analogy and the contribution of the wings and the bulks is computed by means the polar curve of the considered airfoils: AVL provides the wingspan lift coefficient distribution ($C_l(y)$) on each lifting surface.

The airfoil polar functions $C_d = C_d(C_l, M, Re)$ are stored in *AEROSTATE* and the local Mach and Reynolds number are calculated along the wingspan. Thus, it is possible to get the $C_d(y)$ distribution by means of proper interpolations. Finally, $C_{D0_{\text{wing}}}$ is provided by Equation 6 according the definition, i.e:

$$C_{D0_{\text{wing}}} = 2 \frac{\int_0^{b/2} c(y)c_d(y)dy}{S}. \quad (6)$$

5. The software *INTERFACE*

AEROSTATE is a powerful tool to optimize aircraft but it only provides a 2D sketch of the airplane. *INTERFACE* is a software dedicated to link the variables of *AEROSTATE* to *ASD* and, therefore, it is possible to obtain 3D sketches of each aircraft in very quick and iterative way. *INTERFACE* has been developed on Matlab as complementary activity of this work; all details about its possibilities and facilities are given in [12].

6. Research of preliminary optimum configurations

In this section, all the tools previously described are used in order to research optimum configurations. The chosen profile is a six digits NACA airfoil (NACA 642415): it ensures good performances in subsonic conditions because of a large laminar zone. All the PrandtlPlane configuration parameters have been set in *AEROSTATE* referring to Table 1. It is important to remark that the angle of attack of the fuselage (α_{fus}), i.e. the angle between the flow direction and the fuselage axis, is set to zero, in order to minimize the induced drag of the fuselage: in fact, modeling the fuselage as a plane plate, induced drag should be added when α_{fus} increases. Putting $\alpha_{fus}=0$, the model is simpler, the calculation is faster and the fuselage floor is horizontal during cruise. Therefore, the portion of the front wing, which crosses the fuselage, produces no lift. Moreover, the Stability Margin range is set as 0-3%. Finally, the optimization process needs a starting geometry file: it has been set up and loaded by *AEROSTATE* (Figure 8). All details about the starting geometry file can be found in [12]).

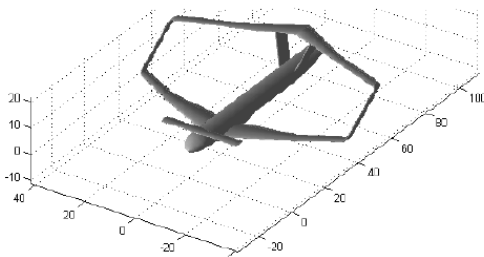


Figure 8. Optimization starting geometry

6.1. Front wing loading variation

The wing loading is an important parameter for an airplane, because it affects performances, aerodynamics and flight mechanics. The computation of the wing loading for conventional airplanes considers the aircraft total weight in a “mission point” (it could be the cruise design point) and the wing surface. In a PrandtlPlane, any lifting surface contributes to the total lift and has a proper wing loading:

$$W/S = \frac{L}{S} \text{ for each wing} \quad (7)$$

In a first analysis, we wish to investigate how the efficiency of the PrandtlPlane freighter depends on the wing loading of the front wing; to do this, we consider

four different optimization, shown in Table 3, in which the wing loading interval is restricted to 200 kg/m^2 on the front wing, meanwhile no strict constraint is given on the rear and auxiliary wings. The improvement of the wing loading increases the aerodynamic efficiency but reduces the structural strength of the wing system and, thus, these analyses allow us to determine a set of optimal solutions to be analyzed in a second step where a structural optimization will be included.

Table 3

Sensitivity to the front wing loading: analysis description

Analysis	W/S [kg/m^2]					
	Front <i>min</i>	Wing <i>max</i>	Rear <i>min</i>	Wing <i>max</i>	Aux. <i>min</i>	Wing <i>max</i>
1	400	600	0	900	0	900
2	500	700	0	900	0	900
3	600	800	0	900	0	900
4	700	900	0	900	0	900

The main results are collected in Figure 9, in which each symbol represents a local optimum or the global optimum. Some configurations are allowed to violate some constraints (this is possible in *AEROSTATE* when the most important constraints are fulfilled, in order to reach quickly the global minima). In this way, interesting configurations are still considered (although they violate some constraints slightly, and will be analyzed afterwards, in a post-processing phase. In summary, the results show that:

- when the front wing loading increases, the auxiliary wing tends to disappear;
- the rear wing solution is scarcely influenced by the front wing loading;
- a high rear wing loading ensures higher efficiency, but the Stability Margin is reduced;
- the rear wing solution depends mainly on the Stability Margin.

6.2. The bulk parameter k_{bulk}

As said before, the general objective function of *AEROSTATE* has been defined as follows:

$$OBJ = -E + k_{bulk}l_{bulk}. \quad (8)$$

In other words, we wish to optimize the aerodynamic efficiency as more as possible and to reduce the bulk

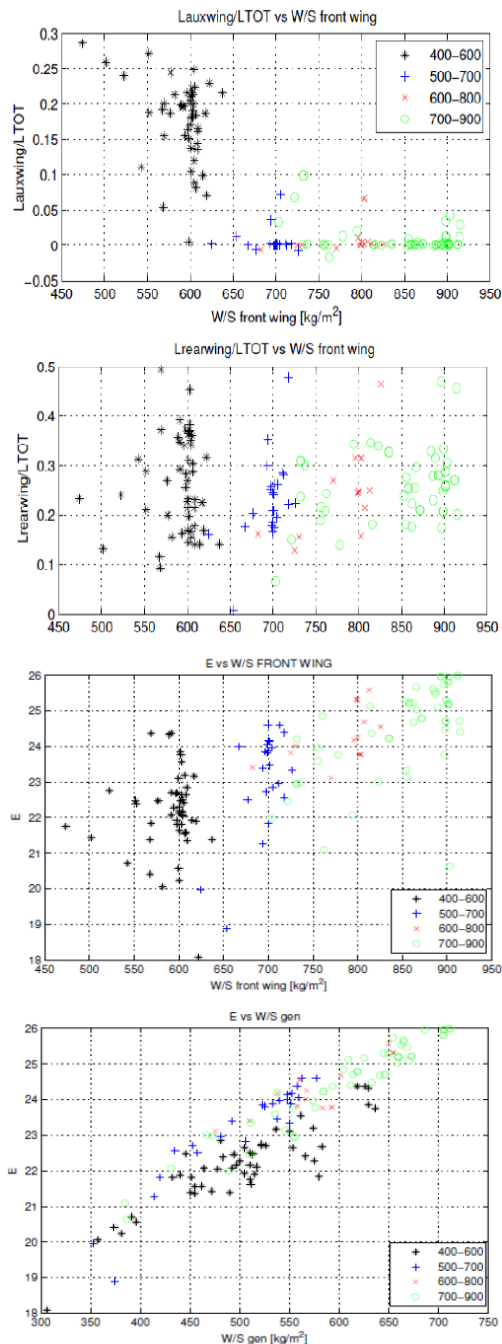


Figure 9. Sensitivity to the front wing loading: Results

length in order to prevent the buckling under the compression loads during cruise. The following analyses have been conducted in order to study the effects of Table 4.

After a sensitivity analysis, the value $k_{bulk} = 0.8$ has been chosen.

Table 4
Sensitivity to the bulk parameter: analysis description

k_{bulk}	0.0 : 0.1 : 1.0	
	W/S [kg/m^2]	
	Lower Boundary	Upper Boundary
	400	600
	300	700
	200	900

6.3. The rear wing loading

The aim of the analyses listed in Table 5 is to find out a suitable range of values for the rear wing loading to reach high efficiency.

Table 5
Sensitivity to the rear wing loading: analysis description

Analysis	W/S [kg/m^2]					
	Front Wing		Rear Wing		Aux. Wing	
	<i>min</i>	<i>max</i>	<i>min</i>	<i>max</i>	<i>min</i>	<i>max</i>
20	400	600	300	600	200	900
21	400	600	400	700	200	900
22	400	600	500	800	200	900

The results show that the front wing lift decreases if the rear wing lift increases and, also, that the aerodynamic efficiency is a slightly growing function of the rear wing loading ([12]). Thus, in summary, the front and the auxiliary wings define the high speed aerodynamic efficiency and the rear wing satisfies both the stability and low speed constraints.

6.4. Influence of wingspan

The wingspan (b) is limited by the hangar sizes and by structural problems, in particular flutter. Results concerning the wingspan sensitivity are collected in Figure 10 and can be summarized as follows: the efficiency increases with the wingspan and, when b decreases, the lift on front is reduced and that on the auxiliary wing increases.

6.5. Rear wing in forward position

This paragraph deals with the effects of moving forward the rear wing, which in turn is connected with the rear wing loading variation. Contrary to the previous analyses, the auxiliary wing does not remain ahead

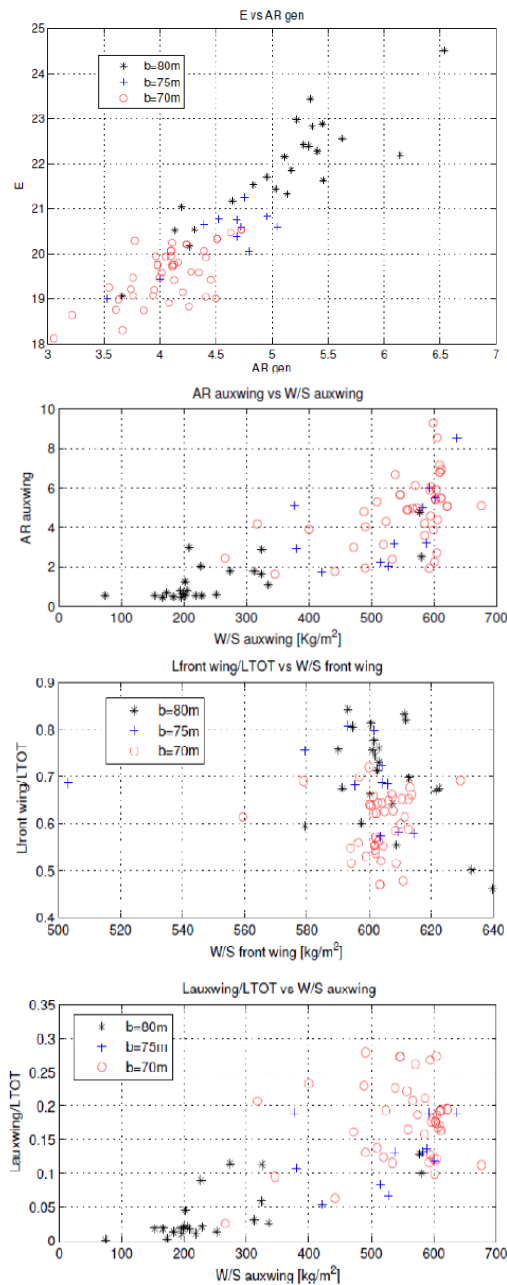


Figure 10. Sensitivity to the wingspan: Results

of the fuselage but moves after the rear wing (Figure 11 shows an example of such an aircraft).

The analyses performed are collected in Table 6.

In the first analysis, the rear wing is moved towards the center of gravity in order to increase its wing loading and the efficiency; in the second analysis, the upper limit of the wing loading of the auxiliary wing is enhanced. The constraint on the Stability Margin is fulfilled by moving the auxiliary wing backwards. The boundaries of the front wing loading are unchanged;

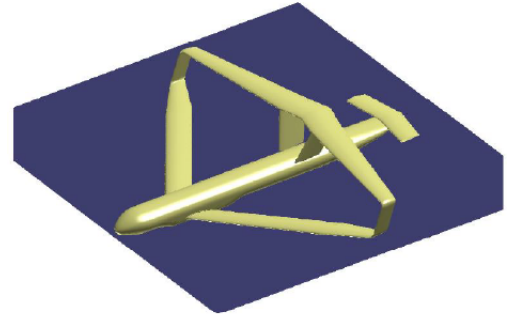


Figure 11. Example of rear wing moved in forward position

Table 6

Rear wing in forward position: analysis description

Analysis Id.	b [m]	H [m]	W/S (min-max) [kg/m^2]		
			Front	Rear	Aux.
1	80	11	400-600	450-750	200-600
2	80	12	400-600	500-800	200-900

thus, the only possibility for the optimization code to satisfy the equilibrium, is to increase the lift of the rear wing (Figure 12).

6.6. The reference analysis

Tables 7, 8 and 9 show some typical configurations obtained.

7. Low speed design

The present paragraph is dedicated to the low speed design. First, with reference to NASA CR 4746 requirements ([16]), the maximum lift during landing is analyzed and the necessary lift coefficient of the whole configuration is computed according to the data in Table 10.

In this preliminary phase, the performances of flaps and slats are studied by applying theoretical and semi empirical formulas, provided by [17].

7.1. High lift devices

The low speed method consists into satisfying the following condition for each wing:

$$\max(C_{l\perp}(y)) \leq C_{l_{\max}}, \quad (9)$$

in which $C_{l\perp}(y)$ is the lift coefficient distribution, evaluated for wing sections perpendicular to isobar curves, and $C_{l_{\max}}$ is the maximum airfoil lift coefficient, calculated according to [17] and [12]). $C_{l\perp}(y)$

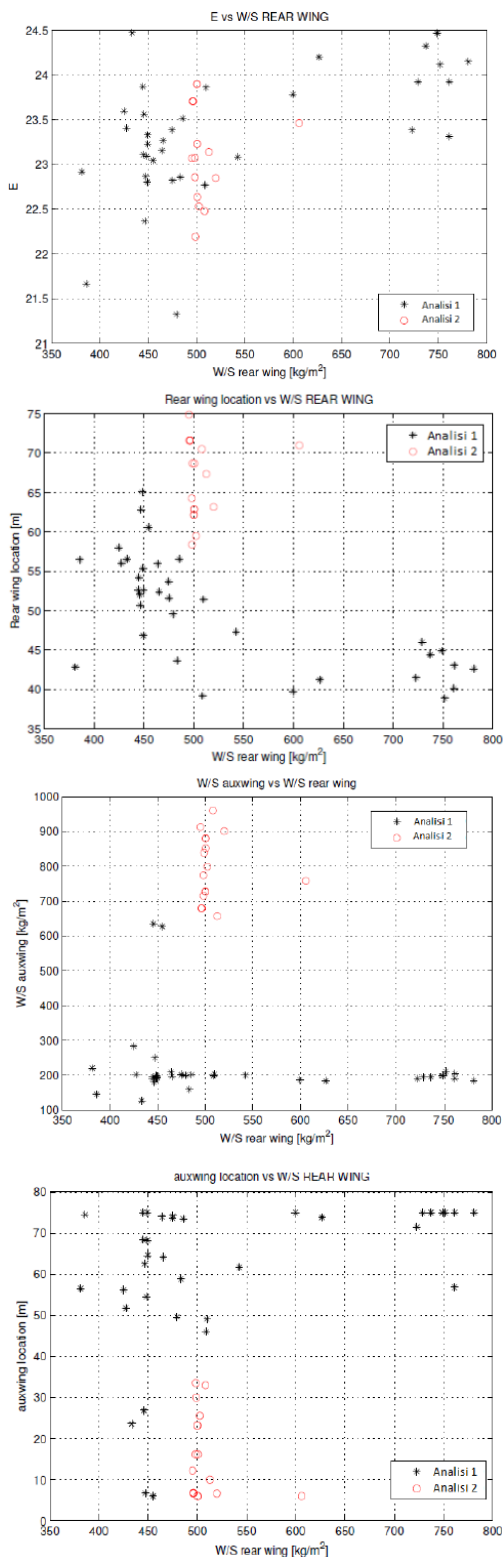
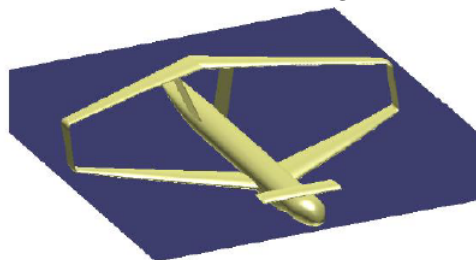


Figure 12. Rear wing in forward position: Results

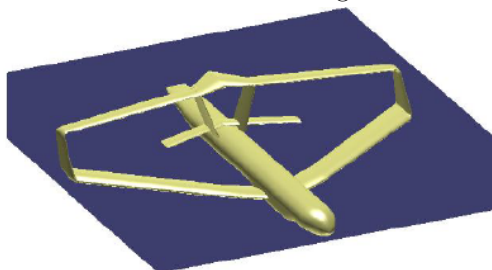
is computed by means of the software AVL, in which all the aerodynamic surfaces and all the wing devices

Table 7
Solution test5trisCurr0: Configuration details



C_L	0.36
C_L front	0.44
C_L rear	0.28
C_L aux.	0.40
E	22.7
SM	1.2%
W/S front [kg/m ²]	601
W/S rear [kg/m ²]	404
W/S aux. [kg/m ²]	581

Table 8
Solution test5trisCurr6: Configuration details

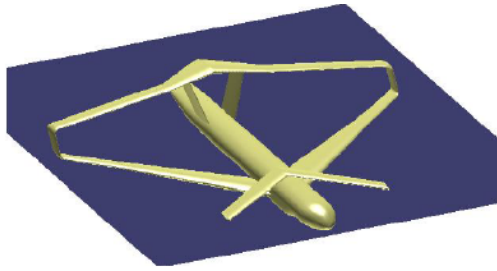


C_L	0.35
C_L front	0.44
C_L rear	0.28
C_L aux.	0.15
E	23.3
SM	-2.4%
W/S front [kg/m ²]	626
W/S rear [kg/m ²]	395
W/S aux. [kg/m ²]	207

(elevators, trailing edge flaps and slats) are modeled; elevators, flaps and slats are represented in AVL as plain flaps and slats. The procedure is iterative.

As a result, the distributions $C_{l\perp}(y)$ are extrapolated and compared with the allowable data values, in

Table 9
Solution test5trisCurr8: Configuration details



C_L	0.37
C_L front	0.42
C_L rear	0.28
C_L aux.	0.41
E	22.2
SM	-0.7%
W/S front [kg/m ²]	601
W/S rear [kg/m ²]	398
W/S aux. [kg/m ²]	584

Table 10
Low speed main quantities

Parameter	Relation/Value
Landing lift coefficient (C_{LS1g})	$0.94^2 1.3^2 C_{L_{appr}}$
Approach lift coefficient ($C_{L_{appr}}$)	$\frac{2W/S}{\rho V_{land}^2}$
Landing Speed (V_{land})	145 kts
Design Landing Weight (W_{land})	$0.75 \cdot MTOW$
Landing Altitude	0 m

order to verify the following conditions on trim:

$$\begin{cases} \frac{|C_{LS1g_{AVL}} - C_{LS1g}|}{C_{LS1g_{AVL}}} \leq 0.05 \\ |C_{m_{AVL}}| \leq 0.03 \end{cases} \quad (10)$$

7.2. Results

The high lift devices of a PrandtlPlane are non conventional: the front wing devices are leading edge slats and trailing edge double slotted flaps; the rear wing has only trailing edge single slotted flaps; the elevator is modeled as a plain flap; the flap and the slat chords are 30% and 15% of the local chord, respectively. Front and rear wings have the same flap deflection.

Different configurations are examined in order to prove that the PrandtlPlane freighter, provided with an auxiliary wing, can satisfy the low speed constraints with many arrangements of the wing system. Some examples are presented in Tables 11-15, where configura-

tions have been already analyzed in cruise conditions, for which aerodynamic efficiency is reported.

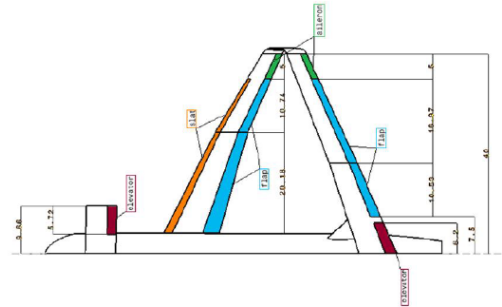
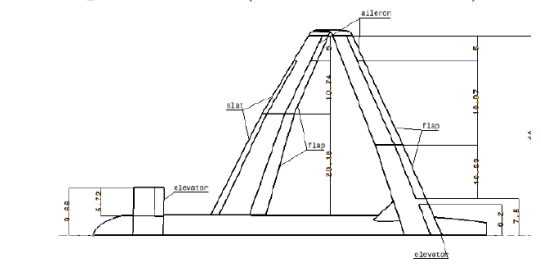


Figure 13. Low speed devices and control surfaces

Table 11
Low Speed Results (Sol. test5trisCurr0)



E_{cruise}	b [m]	S [m ²]
22.7	80	1092
α [deg]	δ_f [deg]	δ_e [deg]
8	22	17

Wing	$C_{l_{max}}$	$\max C_{l_{\perp}}(y)$
Front	3.48	3.43
Rear	2.66	2.26
Aux.	1.20	1.65

8. Conclusions

An optimization procedure has been set up in this work in order to evaluate optimal wing planform that minimize the lift-to-drag ratio. Proper constraints have been considered to take structural requirements and flight mechanics into account. In particular, the wing loading, deriving from both regulation on the landing and from structural reasons, appears the most

Table 12
Low Speed Results (Sol. test5trish75Curr0)

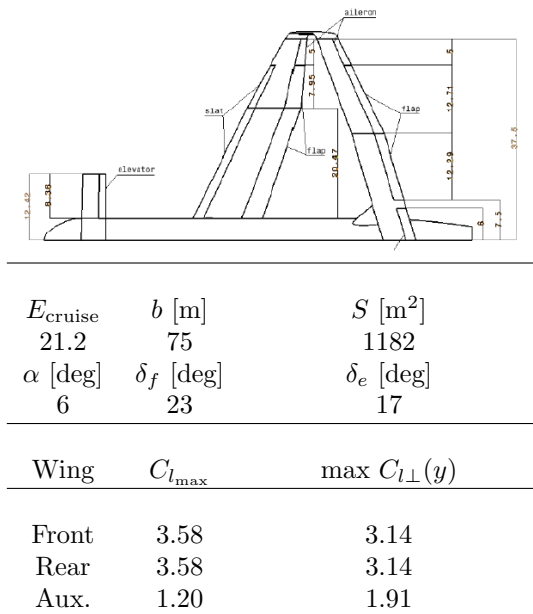
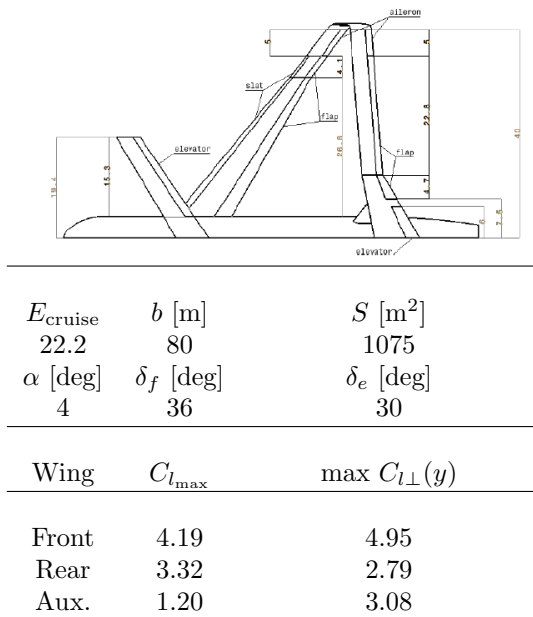


Table 13
Low Speed Results (Sol. test5trisCurr8)



significant parameter, which affects the wing planform. It has been verified that a high front wing loading improves the aerodynamic efficiency E but, at the same time, it makes the front wing overloaded: when the front wing loading is over 700 kg/m², the auxiliary wing is very inefficient, with a small surface and a low lift coefficient. Thus, the fuselage has two supports,

Table 14
Low Speed Results (Sol. test5trisCurr6)

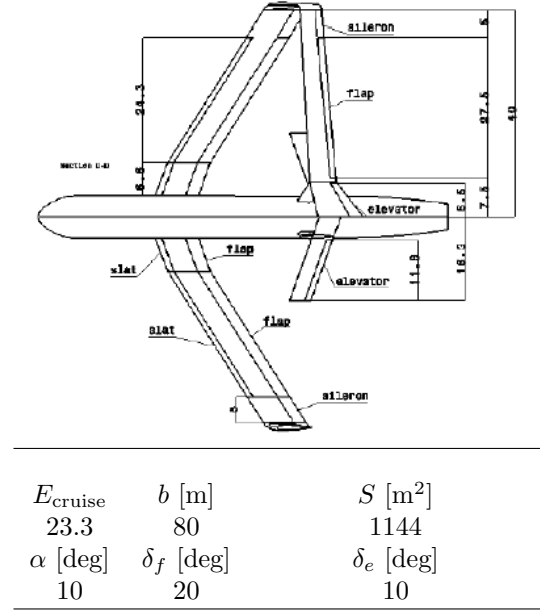
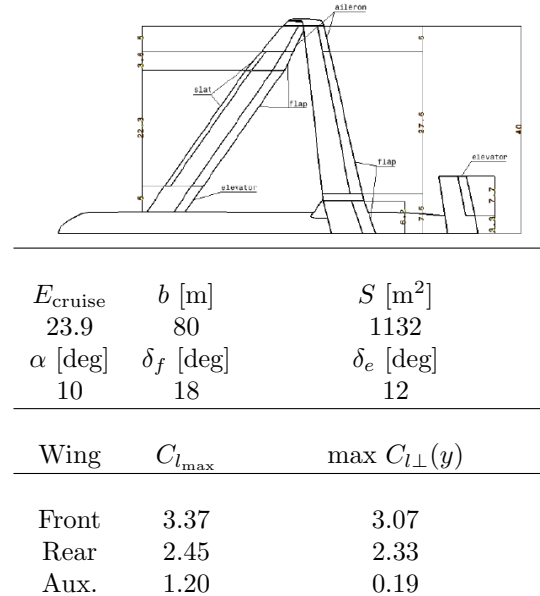


Table 15
Low Speed Results (Sol. test5trish11Curr18)



instead of three, and the bending moment in the fuselage increases.

The rear wing loading has been investigated too. Results underline that when the rear wing loading increases, the response of the aircraft is not unique: on one hand, the rear wing is moved towards the center of gravity (but in this case many configurations do not meet the constraint on the Stability Margin); on the other hand, the rear lift coefficient can be improved. The previous two situations refer to analyses where the auxiliary wing was a canard and its wing loading was limited between 200 kg/m^2 and 900 kg/m^2 . If the upper boundary of the auxiliary wing is cut to 600 kg/m^2 , the optimizer provides new configurations, in which the auxiliary wing is a tail and the rear wing is heavily moved towards the center of gravity and the Stability Margin condition is met by positioning the auxiliary wing backwards, far from the center of gravity. In this case the lateral stability is difficult to be managed with two vertical fins, because they are very close to the center of gravity. Then, the tail can have a “H” shape in order to locate two rudders. Anyway, the efficiency E increases when the rear wing loading increases.

In general, it can be inferred that the most efficient configurations should have three slender lifting surfaces: in fact, it is not sufficient to have a front or rear high Aspect Ratio to improve E .

The bulks length has been taken into account in the objective function by means the parameter k_{bulk} . Bulks have to be sufficiently short because they can undergo buckling. It has been chosen $k_{\text{bulk}} = 0.8$ because it is a compromise value between high efficiency, short bulks, homogeneous distribution of the aerodynamic load on the three wings and not too high C_L .

It has been provided that the height of the two fins (h) does not affect the efficiency in a sensitive manner. Reducing h from 12 m to 11 m or 10 m seems a good solution because the structure is more compact, maintainability is simpler and the wet surface is decreased. However, if the rear wing is closer to the front wing, the downwash effect is stronger and the flow on the rear wing can be slightly spoiled. The aerodynamic efficiency is very sensitive to the wingspan because, when b increases, both the induced drag and the friction drag decrease. Besides, changing the wingspan, the Stability Margin is not influenced. The h/b parameter has been considered and it is observed that the Prandtl’s aerodynamic theory does not comply with the results: in particular, the efficiency is not constant, but it decreases if the wingspan decreases. Again, the wingspan effects are prominent. This behavior is also due to the wing sweep, which are not zero.

From low speed analysis results, it has been verified that the auxiliary wing is actually necessary to meet low speed conditions for the PrandtlPlane freighter. The auxiliary wing works as an elevator that guarantees the trim condition during landing. It should be remarked that the low speed procedure is very pre-

liminary: flaps and slats need to be optimized, taking into account interaction effects. Moreover, in this work, only slotted flaps have been considered. If more expensive Fowler flaps are employed, low speed performances will increase and the two elevators can be less stressed. It is important to remark that many different wings arrangements allow the freighter to land and to meet the low speed constraint. This is a key point in the design process because it demonstrates that the PrandtlPlane freighter with three lifting surfaces is a very versatile aircraft.

Finally, three macro-solutions have been provided by the high speed analysis (optimization process in cruise conditions); they all meet the low speed requirement too. The most remarkable geometric difference is the position of the auxiliary wing along the fuselage. These macro-solutions are shown in Figures 14, 15 and 16.

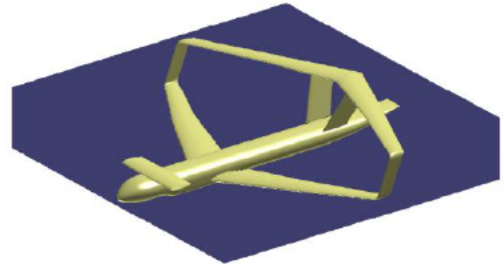


Figure 14. Canard configuration

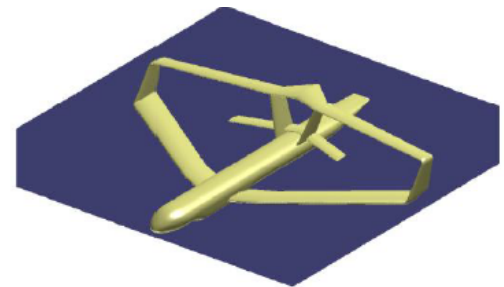


Figure 15. Intermediate configuration

REFERENCES

1. L. Prandtl, “Induced drag of multiplanes”, NACA TN 182, 1924.

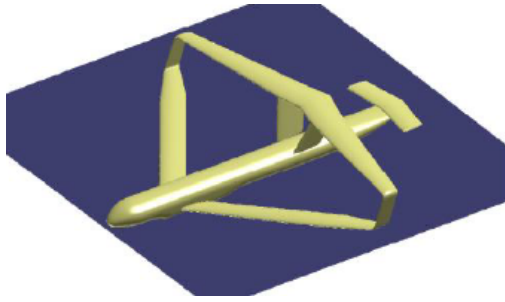


Figure 16. Tail configuration

2. A. Frediani, G. Montanari, M. Pappalardo "Sul problema di Prandtl della minima resistenza indotta di un sistema portante", Atti del XV Congresso Nazionale AIDAA, Torino, Novembre 1999, pag. 267-278.
3. A. Frediani, V. Cipolla, E. Rizzo "The PrandtlPlane Configuration: overview on possible Applications to Civil Aviation" in Springer Optimization and its Applications: Mathematical Challenges for Aerospace Design, Volume 66, Springer, 2012, pp 179-210.
4. R. Cavallaro, L. Demasi, "Challenges, Ideas, and Innovations of Joined-Wing Configurations: A Concept from the Past, an Opportunity for the Future", Progress in Aerospace Sciences, Volume 87, November 2016, Pages 1-93, ISSN 0376-0421, <http://dx.doi.org/10.1016/j.paerosci.2016.07.002>.
5. Cavallaro, R., Bombardieri, R., Demasi, L., Iannelli, A., "Prandtlplane joined wing: Body freedom flutter, limit cycle oscillation and freeplay studies". No. AIAA-2015-1184. 2th SciTech2015, Kissimmee, Florida. URL <http://arc.aiaa.org/doi/abs/10.2514/6.2015-1184>.
6. M. Voskuijl, J. de Klerk and D. van Ginneken "Flight mechanics modeling of the Prandtl plane for conceptual and preliminary design" in "Variational Analysis And Aerospace Engineering: Mathematical Challenges for Aerospace Design", Springer Optimization and its Applications, Volume 66, Springer 2012, pp 463-486.
7. A. Frediani, V. Cipolla, F. Oliviero, "Design of a prototype of light amphibious PrandtlPlane" Scitech-AIAA 2015 Conference , Orlando, USA, January 2015.
8. F. Oliviero, "Conceptual design of a large PrandtlPlane freighter", *M.Sc. Thesis*, Department of Aerospace Engineering, University of Pisa, 2010.
9. A. Rimondi, "Generazione di configurazioni aerodinamiche mediante NURBS. (Non-Uniform Rational B-Splines)", *M.Sc. Thesis*, Department of Aerospace Engineering, University of Pisa, 2004.
10. F. Petri, "Sviluppo del codice A.S.D. per la generazione parametrica di superfici aerodinamiche mediante N.U.R.B.S. (Non-Uniform Rational B-Spline)", *M.Sc. Thesis*, Department of Aerospace Engineering, University of Pisa, 2005.
11. E. Rizzo, "Optimization methods applied to the preliminary design of innovative, non-conventional aircraft configurations", *Ph.D. Thesis*, Department of Aerospace Engineering, University of Pisa, 2009.
12. L. Cappelli, G. Costa, "Aerodynamic optimization of a large PrandtlPlane configuration", *M.Sc. Thesis*, Department of Aerospace Engineering, University of Pisa, 2015.
13. M. Dreha, H. Youngren, "AVL 3.30 User Primer", 2010.
14. V. Cipolla, "Utilizzo di codici a pannelli nel progetto preliminare di velivoli PrandtlPlane ultraleggeri; applicazione a nuove configurazioni", *M.Sc. Thesis*, Department of Aerospace Engineering, University of Pisa, 2006.
15. G. Iezzi, "PrandtlPlane High Lift System Preliminary Aerodynamic Design", *M.Sc. Thesis*, Department of Aerospace Engineering, University of Pisa, 2006.
16. Peter K. C. Rudolph, "High-Lift Systems on Commercial Subsonic Airliners", NASA Contractor Report 4746, 1996.
17. E. Torenbeek, "Synthesis of subsonic Airplane Design", Kluwer Boston Inc., Hingham, 1982
18. R. Marti, "MULTI-START METHODS", Cap. 12 in Handbook of Metaheuristics, F. Glover, G. A. Kochenberger, Kluwer Academic Publishers Group, 2003.
19. D. Zanetti, "Studio preliminare della dinamica libera e delle qualità di volo della configurazione PrandtlPlane", *M.Sc. Thesis*, Department of Aerospace Engineering, University of Pisa, 2013.